Algorithm Theoretical Basis Document (ATBD) Rongowai GNSS-R Level 1a DDM Calibration

Prepared by Xiaoyou Lin

November 14, 2023

(L1 Calibration Algorithm Version: 2.4.)

1 Level 1a Calibration Approach

This document is the first part of the overall Level 1 Calibration Algorithm Theoretical Basis Document (ATBD) describing the Level 1a calibration for the Rongowai Global Navigation Satellite System Reflectometry (GNSS-R) mission which flies a next generation receiver (NGRx) on an Air New Zealand domestic Q300 .

It should be noted that the Rongowai L1a calibration approach differs from the CYGNSS L1a [1] approach in several ways. This is due to the fact that the CYGNSS approach was designed around several limitations of the SGR-ReSI that are not present with the NGRx. The NGRx has 14-bit signal sampling compared to SGR-ReSI's 2-bit. This means that the NGRx hardware front-end gains (inside the Maxim RFIC) can be set to fixed gain levels without concerning about capturing the complete signal and noise within its dynamic range and maintaining the signal's linearity. The NGRx performs 14bit-to-2bit conversion digitally before GNSS processing but also computes statistics about the original 14-bit signal. The SGR-ReSI, on the other hand, had a hardware automatic gain control (AGC) but no observability of its setting. This meant that the CYGNSS receiver AGC needed to be turned off and front-end gain fixed. For CYGNSS, there needed to be a lot of effort for choosing the best gain setting and compensating for quantization effects with 2-bit "bin-ratios" at non-ideal values for different scenarios. This is not needed for the Rongowai L1a calibration.

1.1 Instrument Level 0 Measurement

The Rongowai GNSS-R instrument produces delay-Doppler map (DDM) telemetry packets where the individual bins of the DDM are produced in raw, uncalibrated units referred to as "counts". Within the receiver, these counts are stored as 64-bit unsigned integers. In the telemetry packet, the counts are scaled to 32-bit values. The scale factor, which is common for all bins of all DDMs in the packet, is stored in a separate field.

Level 1a calibration converts each bin in the DDM, which is 40 delay rows times 5 Doppler columns in size, from raw counts to units of watts (defined as power input at a specific port on the Rongowai flight unit enclosure). This conversion requires calibration tables obtained from benchtop measurements, which is described in this document.

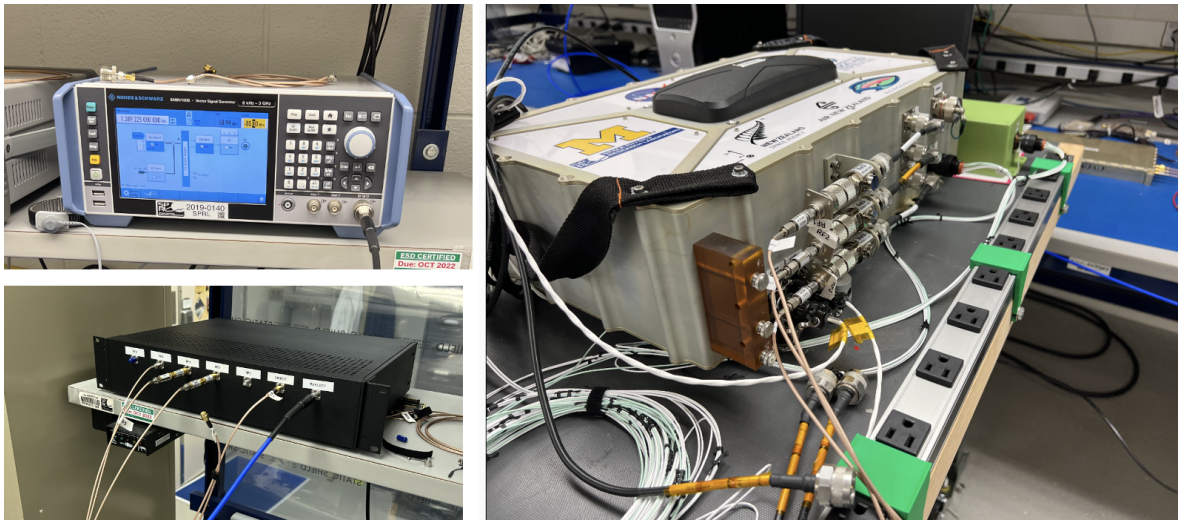

Figure 1: Photos of lab equipment used for calibration, including the signal generator (top left), amplifier box (bottom left), and flight unit (right).

2 L1a Calibration from Counts to Watts

2.1 Collection of Calibration Curves from Lab Measurements

Prior to the installation in the aircraft, the Rongowai flight unit was calibrated on the benchtop using injected GPS signals from a Rhode & Schwarz GNSS signal generator. The generator was configured to output a single GPS L1 CA-coded signal with no dynamics. The signal power was manually adjusted over a range of powers while the NGRx in the flight unit was configured to output DDM counts values. The generated signal was input into a Keysight signal analyzer and its power measured to confirm accuracy of GPS signal power.

The output port of the GNSS signal generator was connected to a box of low-noise amplifiers (LNAs), attenuators and RF power splitters. The box inputs a single signal and outputs 3 signals with approximately 35 dB of gain. Three cables connect the outputs of this box to the 3 RF inputs on the flight unit. Note the 3 RF inputs represent signals coming from the zenith antenna, the nadir antenna left-hand-circularly-polarized (LHCP) channel and the nadir antenna right-hand-circularly-polarized (RHCP) channel, respectively, whereby the latter two contain the science data that are reflected off from the Earth surface. The precise S_{21} gain of all cables and components between the GNSS signal generator and the flight unit input ports were measured at the L1 frequency using a network analyzer and compensated for as part of the calibration. Since the active antenna used by Rongowai also has an internal gain of approximately 35 dB, the range of swept GPS signal powers generated could be made over a realistic range that would be encountered in practice. NGRx 14-bit signal samples indicated that the LNA thermal noise significantly dominated internal noise from the NGRx, allowing L1a calibration to ignore such internal sources and variations. Figure 1 shows photos of the different equipment in the lab during the measurements.

As the calibration took place prior to the availability of the final operational version of the flight software, the NGRx was instead placed into a special calibration mode where it was designed to acquire and closed-loop track a single PRN on all 3 RF input channels,

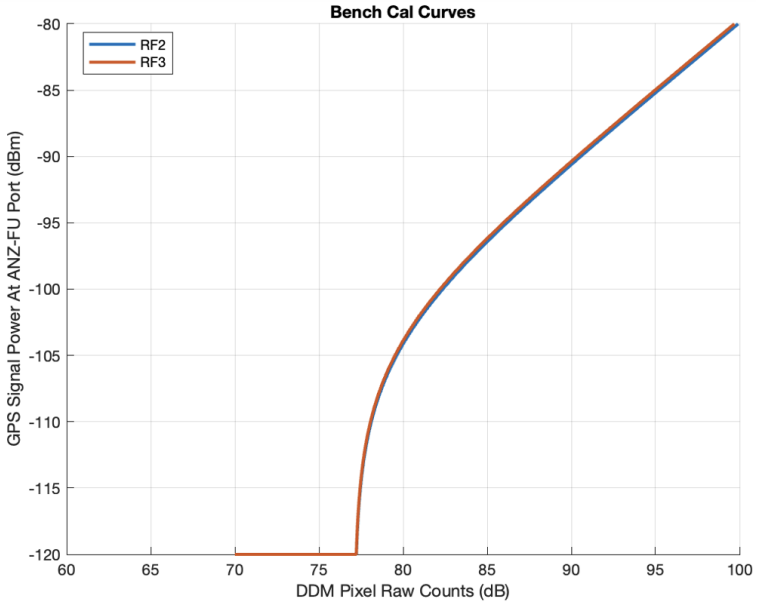

Figure 2: The calibration curves for the Rongowai L1a calibration produced from lab measurements.

simultaneously producing measurements of the signal and noise-floor power levels in the DDM to a log file at 1-Hz for post-processing.

Different input powers were manually typed into the GPS signal generator and held for at least 30 seconds. This produced a sweep of input signal powers. The time-averaged DDM pixel counts of the peak pixel in the DDM was measured vs input signal power at the ANZ Flight Unit Input Port in dBm. Since the bench cal setup prevented measuring very low SNRs, the calibration curves were extended artificially. Figure 2 shows the calibration curves as a map between DDM pixel raw counts to input GPS signal power.

Note that the current L1a calibration curve assumes a "constant" noise floor for all the flights, which will be updated to implement "dynamic" noise floor as one future investigation. In addition, these curves only apply to a specific setting in the 14-bit to 2-bit digital conversion (i.e. the 2-bit "binning thresholds") used by the NGRx during the lab testing. As these binning thresholds will vary during the Rongowai flights, these variations also need to be accounted for. The NGRx field programmable gate array programmable logic (FPGA PL) calculates statistics about the 14-bit signal (mean, standard deviation, bin distributions, etc). The NGRx firmware uses these statistics to calculate the optimal 2-bit binning thresholds and provides these thresholds back to the FPGA PL at 1-Hz to perform the 2-bit binning. There is some optional exponential filtering to keep the binning steady in time, or, alternatively, these binning thresholds can be manually set via commands. Exact binning thresholds that were applied to the data are available in the telemetry. This automatic 2-bit binning is turned on during Rongowai operations for both the science and navigation channels. This keeps the 2-bit binning optimal and prevents any quantization effects from influencing the data in a way that might vary with input noise power. The effect of using this automatic 2-bit binning is that the noise power as measured in 14-bit counts can change, but the noise power measured in 2-bit counts in the DDM remains approximately constant (except when there is radio frequency interference (RFI)).

Complete L1A calibration is performed in three steps:

Step 1: take the DDM pixel values in raw counts (denoted as P_c) and remove the noise floor (N_c) specified in Section 3.

Step 2: use the extended curve in Figure 2(b) to map it into GPS Signal Power at the input to the Rongowai Flight Unit. There is one curve for each RF channel.

Step 3: correct for the NGRx digital signal scaling the 14 to a 2-bit signal. To do this, we take 20*log10 of the 14-bit signal std dev (aka the 2-bit binning threshold) as reported in the DDM packet header. Then, we subtract the binning threshold used during the bench calibration from it to produce a correction.

In the form of an equation, the above process is:

$$\check{P}_d = f_c\big(P_d\big) + 20\ log_{10}(\sigma_c) - \Sigma_c \tag{1}$$

where $\check{P}_d$ is the calibrated DDM bin value in units of dBm, and $P_d = P_c - N_c$ is the DDM bin value measuerd in raw counts after the noise floor has been removed. Subscript c is used to indicate the RF channel index (1, 2 or 3) on the Rongowai Flight Unit enclosure. Note that only RF channels 2 and 3 contain scientific products. The function f_c is the calibration curve corresponding to the RF channel c, with an input parameter of P_d, σ_c is the binning threshold (in absolute units of counts) of the cth RF channel from the DDM packet header, and Σ_c is the binning threshold used during bench-top calibration in the lab, which is 49.6 dB and 50.4 dB for RF channel 2 and 3, respectively. Consequently, $\check{P}_d$ is the L1a product which will be used as the input to derive normalised bistatic radar cross section (NBRCS) and reflectivity in L1b.

This calibration is meant to produce power input at the port of the flight unit. To convert this signal power at port of Air New Zealand flight unit to incident signal power on the antenna will require several additional pieces of information. First, the loss in the cables connecting the aircraft antennas to the flight unit, which were measured onsite during installation. Second is the active antenna realized gain patterns with nominal (i.e. warm) internal LNA gain. This antenna data was collected using chamber measurements of the exact Rongowai antennas prior to installations. Third are the gain variations of the LNAs in the antennas as a function of LNA temperature. This was characterized using bench measurements of a deconstructed antenna. Finally, a thermal model is needed to relate temperatures measured by probes on outside of antenna to the antenna LNA temperature internally. The first and second measures will be presented in L1b calibration ATBD, whereas the third and fourth measures require a model that will be developed in later versions of the calibration.

2.2 Discrepancy Between Calibrated and Modelled Results

To validate the calibrated power, the results are compared with the modeled results here. Coherent reflection of GPS signal from a relatively smooth surface of inland water body is compared with a coherent reflection model to calibrate the 1) dual-polarized antenna pattern and 2) GNSS-R cross-polarized power measurement.

2.2.1 Model Methodology

Equation (2) shows the matrix form of the Friis transmission formula to account for the coherent dual-pol signal reflection through the specular point,

$$\begin{bmatrix} P_L \\ P_R \end{bmatrix} = \frac{\lambda^2}{(4\pi)^2} \cdot \frac{1}{(R_1+R_2)^2} \begin{bmatrix} G_{LL} & G_{LR} \\ G_{RL} & G_{RR} \end{bmatrix} \begin{bmatrix} \mathcal{R}_{LR} & \mathcal{R}_{LL} \\ \mathcal{R}_{RR} & \mathcal{R}_{RL} \end{bmatrix} \begin{bmatrix} E_R^{GNSS} \\ E_L^{GNSS} \end{bmatrix} |\chi|^2 \tag{2}$$

where P is the received power, E is GPS effective integrated radiated power (EIRP), R is range, G is receiver antenna gain, R_1 and R_2 are distance between Transmitter to Specular and Receiver to Specular respectively, G is the NGRx receiver antenna gain, $\mathcal{R}$ is surface reflectivity, χ accounts for the scattering loss caused by surface roughness, and the subscripts denote the polarization state (L for LHCP, R for RHCP) of the signal.

In the model, R_1 and R_2 can be found in L1 file variables `rx_to_sp_range` and `tx_to_sp_range`. The NGRx antenna LHCP & RHCP Co-pol & Cross-pol gains were measured in ElectroScience Lab (ESL), The Ohio State University. Their values can be found either from L1 file variables `sp_rx_gain_copol` and `sp_rx_gain_xpol`, or by interpolating the original antenna measurement data with the direction of the arrived signal in the antenna body frame (`sp_theta_body` and `sp_az_body`). The co-pol GPS EIRP (E_R^{GNSS}) has previously been measured for the CYGNSS mission [2]. Currently the cross-pol GPS EIRP (E_L^{GNSS}) is assumed to be zero, but it will be changed later as the measurement of GPS Cross-pol EIRP experiment is still in progress. This will be further discussed in Rongowai's L1b ATBD.

The surface Fresnel reflectivity in polarization LR/RL (Co-pol) and LL/RR (X-pol) are:

$$\mathcal{R}_{LR} = \mathcal{R}_{RL} = \left| \frac{1}{2}(\mathcal{R}_{VV} - \mathcal{R}_{HH}) \right|^2 \tag{3}$$

$$\mathcal{R}_{LL} = \mathcal{R}_{RR} = \left| \frac{1}{2}(\mathcal{R}_{VV} + \mathcal{R}_{HH}) \right|^2 \tag{4}$$

where

$$\mathcal{R}_{VV} = \frac{\epsilon \cos\theta_i - \sqrt{\epsilon - \sin^2\theta_i}}{\epsilon \cos\theta_i + \sqrt{\epsilon - \sin^2\theta_i}} \tag{5}$$

$$\mathcal{R}_{HH} = \frac{\cos\theta_i - \sqrt{\epsilon - \sin^2\theta_i}}{\cos\theta_i + \sqrt{\epsilon - \sin^2\theta_i}} \tag{6}$$

Note that $\mathcal{R}_{HH}$ and $\mathcal{R}_{VV}$ are functions of incidence angle θ_i (L1 variable `sp_inc_angle`) and surface relative complex permittivity ϵ. For water surface, ϵ can be obtained through a microwave sea dielectric model [3] as a function of salinity, temperature, and frequency. For inland water body, 0 salinity and 20 $^\circ C$ are assumed.

The scattering loss caused by surface roughness is directly related to water body surface windspeed. Due to roughness, the received coherent power at the specular direction is attenuated by a factor [4]

$$|\chi|^2 = \exp\left(-4R_a^2\right) \tag{7}$$

where the Rayleigh parameter

$$R_a = \pi H_s \cos\left(\theta_{inc}\right)/(2\lambda) \tag{8}$$

where H_s is the significant wave height which depends on wind speed, water depth and fetch, and θ_{inc} is the incidence angle (L1 variable `sp_inc_angle`). For H_s, CERC empirical model [5] is used:

$$H_s = \frac{U_A^2}{g} 0.283 \tanh\left[0.53\left(\frac{g \cdot d}{U_A^2}\right)^{\frac{3}{4}}\right] \cdot \tanh\left\{\frac{0.00565\left(\frac{g \cdot F}{U_A^2}\right)^{\frac{1}{2}}}{\tanh\left[0.53\left(\frac{g \cdot d}{U_A^2}\right)^{\frac{3}{4}}\right]}\right\} \tag{9}$$

In this equation, $U_A = 0.71 U_{10}^{(1.23)}$, where U_{10} is the windspeed 10 m above water surface. g is the gravitational acceleration (m/s^2), d is the water depth (m), and F is the Fetch (m).

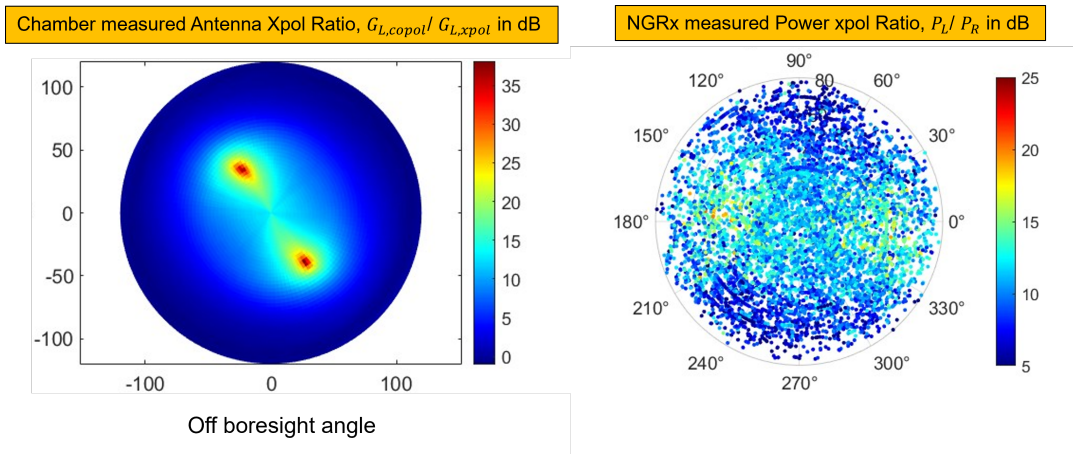

Figure 3: Left: Chamber measured NGRx antenna Xpol ratio at 1.575 GHz; Right: NGRx measured power cross-pol ratio. Both are plotted in antenna polar plot (radius: off boresight angle; polar angle: azimuth angle) and in dB scale

2.2.2 Model vs Measurement

Antenna Pattern

The chamber measured antenna cross-pol ratio is plotted in figure 3 left. For signal reflected from inland water body surface, if assume low cross-pol reflectivity, low cross-pol EIRP, then $P_L/P_R \approx G_{L,copol}/G_{L,xpol}$. However, the NGRx measured power cross-pol power ratio plotted in figure 3 right indicates that the antenna pattern is rotated. The measured power is obtained from samples whose specular surface types (L1 variable `sp_surface_type`) are labeled as inland water body during 11/1/2022 to 3/11/2023. We will further present the implementation of the antenna pattern in Rongowai's L1b ATBD.

Dual-channel Power

The model described in the previous section is used to predict coherent reflected power from the **Lake Taupo** and compare with the NGRx flight measurement during the calibration period from 11/1/2022 to 3/11/2023. Figure 4 shows the satellite map of Lake Taupo from Google Earth. The lake surface windspeed is measured and recorded hourly in the Turangi 2 EWS (#25643) station which is labeled in Figure 4. Data is available on the NIWO Cliffo Service

Website (https://cliflo.niwa.co.nz/). A mean lake surface windspeed of 2.97 m/s averaged over the calibration period, a mean water depth of 110 m, and a mean fetch of 2000 m (a random number, but a reasonable guess) are input into the CERC model to calculate the significant wave height and scattering loss. With other parameters, P_L and P_R in equation (2) can be estimated.

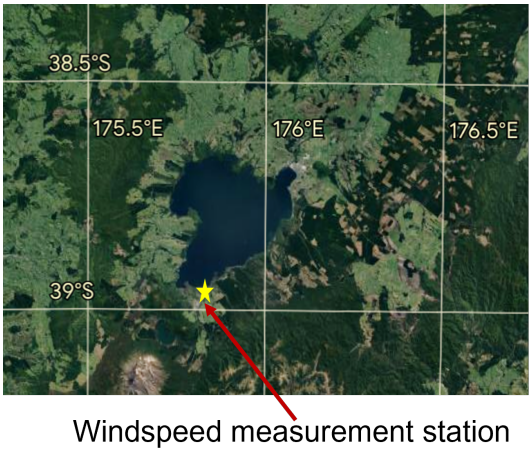

Figure 4: Lake Taupo. The windspeed measurement station at the south coast is labeled. Source: Google Earth

Measured NGRx dual-pol power is obtained by indexing the specular bins of LHCP & RHCP DDMs (L1 Variables: power DDM: `L1a_power_ddm`, SP index: `brcs_ddm_sp_bin_delay_row`, `brcs_ddm_sp_bin_dopp_col`). Filtering conditions are also applied to the Rongowai measurement data. Data satisfying the following conditions is excluded:

- flight altitude (L1 variable `ac_alt`) $< 0.9 \times$ flight peak altitude
- LHCP DDM SNR (L1 variable `ddm_snr`) < 2 dB

The first condition filters out data obtained when the flight was taking off or landing; the second condition filters out data near coast line since SNR is expected to be larger with less land contamination (the number is random but a reasonable guess); the third condition filters out data obtained when the flight was turning its direction, which induce yaw and roll angles uncertainty.

The histograms of modeled and measured specular coherent power reflected from Lake Taupo are plotted in figure 5. A bias is clearly observed between model and measurement in both LHCP and RHCP channels.

3 Noise Floor and Signal-to-Noise Ratio

Every DDM includes a number of bins where signal power does not present and DDM noise floor level can be estimated. These bins physically represents delays above the land or ocean surface, which provide an estimate of the DDM noise power.

Rongowai has been set to track 10 GPS-reflected signals in the reflection mode from the LHCP nadir antenna port and the same 10 in from the RHCP port. Consequently, the 10

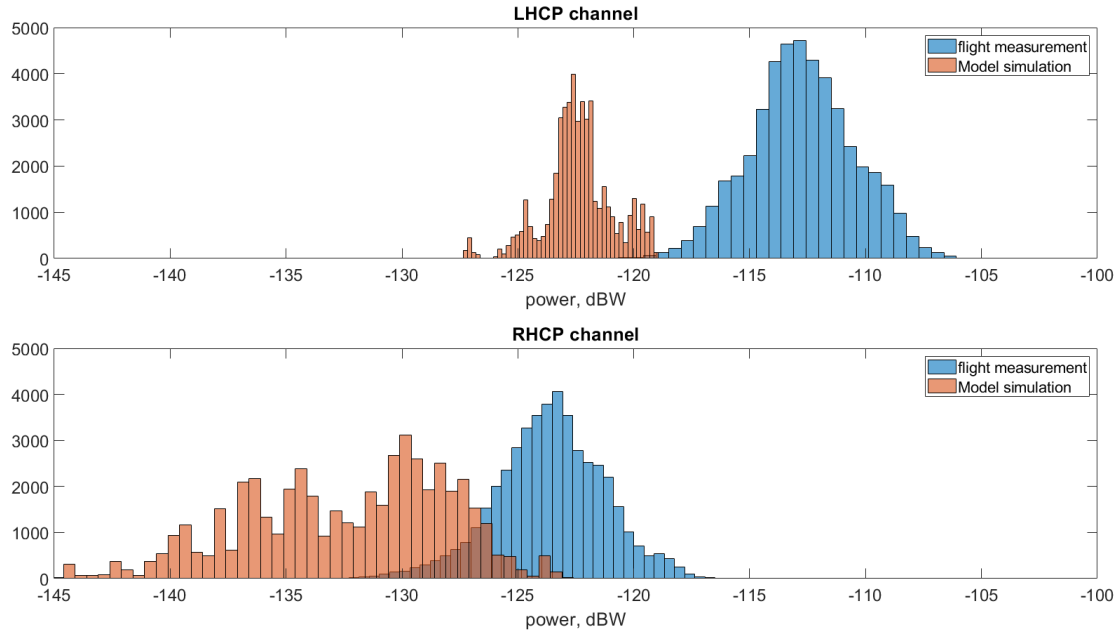

Figure 5: NGRx measrued power (blue) vs modeled power (orange). Upper: LHCP co-pol channel; Lower: RHCP cross-pol channel

LHCP DDMs collected at the same timestamp can share the same noise floor, likewise for the 10 RHCP DDMs from the same timestamp.

At this stage, to minimise the uncertainties of noise floor due to the fluctuation of specular points on complex topography, one single LHCP noise floor is derived for all the LCHP DDMs from the entire flight, whereas one single RHCP noise floor is derived for all the RHCP DDMs. Below are the detail steps to estimate LHCP and RHCP noise floors:

1) Deriving the theoretical row index of the SP for each DDM. This derivation will be presented in L1b ATBD.

2) Selecting all the LHCP/RHCP DDMs whose specular bin is at least 10 delay rows away from the DDM bottom (i.e., delay row 39).

3) For each DDM that meet the requirement set in step (2), deriving their noise floors by averaging the DDM counts value from all the delay-Doppler bins in the fist 5 delay rows.

4) The noise floor C_N for all the LHCP/RHCP DDMs from this flight is the median value of all the noise floors obtained in step (3).

Consequently, the signal-to-noise ratio (SNR) of a DDM is given by:

$$SNR = \frac{P_{SP} - N}{N}, \tag{10}$$

where P is the DDM values in raw counts at the pixel that includes the specular point.

References

[1] O. M. Gleason, Ruf, "The cygnss level 1 calibration algorithm and error analysis based on on-orbit measurements," *IEEE Journal of Selected Topics in Applied Earth Observations*

and Remote Sensing, vol. 12(1), pp. 37–49, 2018.

[2] T. Wang, C. S. Ruf, B. Block, D. S. McKague, and S. Gleason, "Design and performance of a gps constellation power monitor system for improved cygnss l1b calibration," *IEEE Journal of Selected Topics in Applied Earth Observations and Remote Sensing*, vol. 12, no. 1, pp. 26–36, 2019.

[3] L. Klein and C. Swift, "An improved model for the dielectric constant of sea water at microwave frequencies," *IEEE Transactions on Antennas and Propagation*, vol. 25, no. 1, pp. 104–111, 1977.

[4] E. Loria, A. O'Brien, V. Zavorotny, and C. Zuffada, "Towards wind vector and wave height retrievals over inland waters using cygnss," *Earth and Space Science*, vol. 8, no. 7, p. e2020EA001506, 2021.

[5] E. Loria, A. O'Brien, V. Zavorotny, and C. Zuffada, "Towards Wind Vector and Wave Height Retrievals Over Inland Waters Using CYGNSS," *Earth and Space Science*, vol. 8, no. 7, p. e2020EA001506, 2021. _eprint: https://onlinelibrary.wiley.com/doi/pdf/10.1029/2020EA001506.